Carbohydrate Polymers 101 (2014) 574–581

Contents lists available at ScienceDirect

Carbohydrate Polymers

journal homepage: www.elsevier.com/locate/carbpol

Peach gum for efficient removal of methylene blue and methyl violet dyes from aqueous solution

Li Zhou*, Jiachang Huang, Benzhao He, Faai Zhang, Huabin Li

Guangxi Scientific Experiment Center of Mining, Metallurgy and Environment, and College of Material Science and Engineering, Guilin University of Technology, Guilin 541004, PR China

ARTICLE INFO

Article history:
Received 18 June 2013
Received in revised form
10 September 2013
Accepted 27 September 2013
Available online 5 October 2013

Keywords:
Peach gum
Adsorption
Dye
Methylene blue
Methyl violet

ABSTRACT

This study investigated the potential use of natural peach gum (PG) as alternative adsorbent for the removal of dyes from aqueous solutions. The PG showed high adsorption capacities and selectivity for cationic dyes (e.g., methylene blue (MB) and methyl violet (MV)) in the pH range 6–10. 98% of MB and MV could be adsorbed within 5 min, and both of the adsorptions reached equilibrium within 30 min. The dye uptake process followed the pseudo-second-order kinetic model. The intraparticle diffusion was not the sole rate controlling step. Equilibrium adsorption isotherm data indicated a good fit to the Langmuir isotherm model. Regeneration study revealed that PG could be well regenerated in acid solution. The recovered PG still exhibited high adsorption capacity even after five cycles of desorption–adsorption. On the basis of its excellent adsorption performance and facile availability, PG can be employed as an efficient low cost adsorbent for environmental cleanup.

1. Introduction

Dyes are widely used in industrial fields such as textile, printing, paper-making, plastic, coating and food. It has been reported that 10–15% of the dye is released to the environment after dyeing process (Chowdhury, Mishra, Saha, & Kushwaha, 2011). Because the dye effluent may cause damage to aquatic biota and human by mutagenic and carcinogenic effects, the removal of dye pollutants from wastewater is of great importance (Crini, 2006). Various removal methods, including adsorption (Fan et al., 2012; Ngah, Teong, & Hanafiah, 2011), coagulation (Slokar & Le Marechal, 1998), membrane filtration (Madaeni, Jamali, & Islami, 2011) and advanced oxidation (Serpone, Horikoshi, & Emeline, 2010), have been employed to eliminate dyes from wastewaters. Among them, adsorption has been recognized as a promising technique due to its high efficiency, simplicity of design, ease of operation as well as the wide suitability for diverse types of dyes (Asgher & Bhatti, 2012; Dotto & Pinto, 2011).

During the past decades, activated carbon (AC) is the most commonly used adsorbent. However, the AC suffers from some drawbacks such as high cost, difficult disposal and regeneration (Dutta, Bhattacharyya, Ganguly, Gupta, & Basu, 2011). Recently, increasing attention was paid on the development of highly effective and low cost adsorbents (Aksu, 2005; Gupta & Suhas, 2009; Rafatullah, Sulaiman, Hashim, & Ahmad, 2010). In this respect, renewable biological adsorbents (also called bioadsorbents) are attractive because of their low cost, easy availability and low toxicity. Various renewable materials, such as rice husk (Vadivelan & Kumar, 2005; Zou, Li, Bai, Shi, & Han, 2011), castor seed shell (Oladoja, Aboluwoye, Oladimeji, Ashogbon, & Otemuyiwa, 2008), banana peel (Annadurai, Juang, & Lee, 2002), wheat shell (Bulut & Aydin, 2006) and peanut hull (Gong, Li, Yang, Sun, & Chen, 2005), have been used as adsorbent for the removal of dye from aqueous solution. However, most of the reported bioadsorbents show low adsorption capacity, which significantly limits their practical applications. Therefore, exploring new bioadsorbents that are more effective, eco-friendly and cost-effective is highly desired.

Peach gum (PG), a kind of gum exudate, is produced as a result of physiological process or mechanical injury of peach tree (*Prunus persica*, family Rosaceae) (Simas-Tosin et al., 2009). PG is a kind of abundant natural biomass in many areas of the world. It is reported that more than 10 billion tons of PG are yielded in China annually (Xie & Ren, 2008). The composition and structure of PG have been studied (Fernanda et al., 2008; Simas et al., 2008). The main composition of PG is acidic polysaccharide that generally consists of galactose (42%), arabinose (36–37%), uronic acid (7–13%), xylose (7%) and mannose (2%) (Fernanda et al., 2008; Simas et al., 2008). Because PG polysaccharide possesses high molecular weight and highly branched molecular structure, it is insoluble in aqueous solution. In view of its unique composition and property, PG

* Corresponding author. Tel.: +86 773 589 6438; fax: +86 773 589 6671.
E-mail address: zhouli@glut.edu.cn (L. Zhou).

0144-8617/$ – see front matter © 2013 Elsevier Ltd. All rights reserved.
http://dx.doi.org/10.1016/j.carbpol.2013.09.093

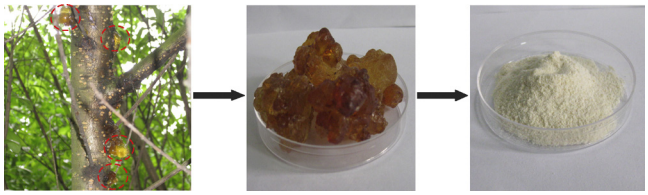

Fig. 1. Photographs of crude PG and dried PG powder.

should be a promising adsorbent for the removal of cationic dyes from wastewater. On one hand, PG contains numerous negatively charged carboxylic groups that can adsorb cationic dyes through strong electrostatic interactions. According to our previous studies, adsorbent with high content of charged functional groups possesses high adsorption capacity (Chen, Zhou, Zhang, Yu, & Wei, 2012; Zhou, Gao, & Xu, 2010). On the other hand, PG can be easily separated from aqueous solution after adsorption. Despite PG has been studied for applications in medicine, printing, fluorescent materials, cosmetic and food industries (Xie, Zhou, & Qian, 2006; Zhou, He, & Huang, 2013), the use of PG as adsorbent for treatment of organic pollutants has not been reported.

Therefore, the objective of this work is to explore the potential of PG as low cost adsorbent for the removal of dyes from aqueous solutions. The influences of adsorption parameters such as initial dye concentration, contact time, solution pH and ionic strength on the adsorption performance of PG were investigated. The new adsorbent is proven effective in removal of cationic dyes. The adsorption mechanism of PG adsorbent was discussed in detail. The regeneration of the dye-adsorbed PG was also studied.

2. Materials and methods

2.1. Materials

The crude peach gum from the peach tree (*P. persica*) trunk was collected at Zizhou Park (Guilin, China). The dried crude PG was grounded into powder (Specific surface area: $15 \pm 5\ m^2/g$) before adsorption application (Fig. 1). Congo red (CR), methylene blue (MB), methyl orange (MO) and methyl violet (MV) were purchased from Aladdin Chemistry Co. Ltd. (Shanghai, China). The structure and characteristics of the used dyes are presented in Table 1. Deionized water was used as solvent throughout the experiments. All other reagents were used as received without further purification.

2.2. Adsorption of dye solution

The adsorption of dyes on PG was performed in a batch system. Typically, 20 mg of PG powder was added to 10 mL of dye solution of known concentration. The solution pH was adjusted with NaOH (0.1 M) or HCl (0.1 M). The mixture was agitated at 100 rpm/min at 25 °C. In order to ensure that adsorptive equilibrium was reached, the agitation was carried out for 24 h. The samples were withdrawn from the experimental flask at predetermined time interval until adsorption equilibrium was achieved. The dye solution was separated from the adsorbent by centrifugation at 5000 rpm/min for 5 min. The supernatants were then filtered to ensure that the solutions were free from PG particles before measuring the residual dye concentration. All adsorption experiments were carried out in triplicate, and the average values were used to minimize random error.

Dye concentration was determined by UV–vis spectrophotometer. Calibration curves were plotted between absorbance and concentration of the standard dye solutions. It should be pointed that the intensity of absorption peaks of MB and MV solutions at low pH (e.g. 3–4) or high pH (e.g., 9–10) are slightly changed as compared with those of solutions in the pH range 5–8. Calibration curves were plotted between absorbance and concentration of the standard dye solutions at different pH values. In addition, no pH change is observed during experiments. The amount of dyes adsorbed at equilibrium was calculated from the following mass balance equation:

$$Q_e = \frac{(C_0 - C_e)V}{m} \quad (1)$$

where Q_e ($mg\,g^{-1}$) is the amount of dye adsorbed per gram of adsorbent at equilibrium, C_0 ($mg\,L^{-1}$) is the initial concentration of dye in the solution, C_e ($mg\,L^{-1}$) is the concentration of dye at equilibrium, V (L) is the volume of the solution, and m (g) is the mass of the adsorbent used. It is noted that the adsorption capacity has been corrected with the pure products.

2.3. Selective adsorption of cationic dye from dye mixture

The selective adsorption experiments were conducted in the mixture of MB and MO at pH 7.0. In a typical procedure, 20 mg of PG powder was added to 10 mL of mixed MB and MV solution. The initial concentration of MB and MO are 0.5 mM. After stirring at 100 rpm/min at 25 °C for 0.5 h, the dye solution was separated by centrifugation. The dye concentration in the solution and the removal of dye were traced and determined by UV–vis spectra.

2.4. Adsorbent regeneration

Desorption of dye was performed by putting the dye-adsorbed PG into 40 mL of HCl solution (0.05 M). The suspension was stirred for 2 h. Subsequently, the PG adsorbent was collected by centrifugation. After washing with water, the PG was reused for adsorption again. The supernatant solution was analyzed by UV–vis spectrophotometer.

2.5. Analytical methods

Fourier transform infrared (FTIR) spectra were measured on a Thermo Nexus 470 FTIR spectrometer (KBr disk). Absorption spectra were recorded on a UV-3600 UV–vis spectrophotometer (Shimadzu). Optical microscope image was obtained using an optical microscope (LEICADM RXP) with imaging software. The zeta potential values of the PG at various pH values were obtained with a zeta potential analyzer (Zetasizer Nano ZS90, Malvern). The specific surface area was determined by BET-N_2 adsorption method by using a Quantachrome NOVA 1200e Series at 77.35 K.

3. Theory

3.1. Adsorption kinetics

To study the time dependence of adsorption process and further investigate the adsorption mechanisms, two well-known kinetic models were used to fit the adsorption date, namely pseudo-first-order and pseudo-second-order models (Bulut & Aydin, 2006).

$$\text{Pseudo-first-order equation}: \ln(Q_e - Q_t) = \ln Q_e - k_1 t \quad (2)$$

$$\text{Pseudo-second-order equation}: \frac{t}{Q_t} = \left(\frac{1}{k_2 Q_e^2}\right) + \frac{t}{Q_e} \quad (3)$$

where Q_t ($mg\,g^{-1}$) is the amount of dye adsorbed at the time t (min), k_1 (min^{-1}) is the pseudo-first-order rate constant, k_2 ($g\,mg^{-1}\,min^{-1}$) is the pseudo-second-order rate constant.

Table 1
Structure and characteristics of the used dyes.

Dye	Chemical structure	Color index number	λ_{max} (nm)	Molecular weight (g mol^{-1})
MB	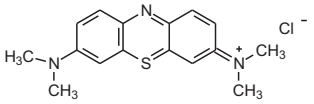	52,015	662	373.90
MV	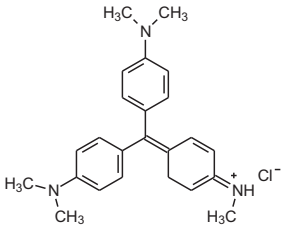	42,535	583	407.99
CR	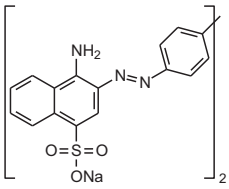	22,120	496	699.66
MO	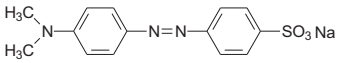	13,025	463	327.33

Since the above kinetic models cannot describe the intraparticle diffusion, the intraparticle mass transfer diffusion model (Weber & Morris, 1963) was also studied.

$$\text{Intraparticle diffusion}: Q_t = k_i t^{0.5} + C \quad (4)$$

where k_i (mg g^{-1} min$^{-1/2}$) is the intraparticle diffusion rate constant, C (mg g^{-1}) is the intercept.

3.2. Adsorption isotherms

Isotherms studies can describe how the adsorbates interact with adsorbents, which is the most important parameter for designing a desired adsorption system. Three famous models were used in current study to describe the adsorption process including Freundlich, Langmuir and Dubinin-Radushkevich (D-R) isotherm models (Vadivelan & Kumar, 2005).

$$\text{Freundlich isotherm}: \ln Q_e = \ln K_F + b_F \ln C_e \quad (5)$$

$$\text{Langmuir isotherm}: \frac{C_e}{Q_e} = \frac{C_e}{Q_{max}} + \frac{1}{Q_{max} K_L} \quad (6)$$

$$\text{Dubinin} - \text{Radushkevich (D} - \text{R)}: \ln Q_e = \ln Q_0 - K_{DR}\varepsilon^2 \quad (7)$$

$$\varepsilon = RT \ln\left(1 + \frac{1}{C_e}\right) \quad (8)$$

where K_F is the Freundlich constant, b_F is a constant depicting the adsorption intensity, Q_{max} (mg g^{-1}) is the maximum adsorption capacity of the adsorbent, K_L (L mg^{-1}) is the Langmuir adsorption constant, K_{DR} (mol^2 kJ^{-2}) is the D–R isotherm constant, ε (kJ mol^{-1}) is Polanyi potential, Q_0 (mg g^{-1}) is adsorption capacity derived from the intercept of lnQ_e versus $-\varepsilon^2$, R is universal gas constant (8.314 J mol^{-1} K^{-1}) and T (K) is Kelvin temperature.

The K_L from Langmuir adsorption isotherm is employed to predict the favorability of adsorption process (Hameed, 2008).

$$R_L = \frac{1}{1 + K_L C_0} \quad (9)$$

where R_L is a dimensionless constant separation factor. Adsorption isotherm is considered to be favorable ($1 > R_L > 0$), linear ($R_L = 1$), unfavorable ($R_L > 1$) or irreversible ($R_L = 0$) on the basis of the value of R_L. In addition, the *D–R* model is mainly used to estimate the average free energy of adsorption *(E)*, which is expressed using the following equation (Saha, Das, Saikia, & Das, 2011):

$$E = \frac{1}{\sqrt{2K_{DR}}} \quad (10)$$

The value of E can characterize the type of adsorption as chemical adsorption ($E = 8$–16 kJ mol^{-1}) or physical adsorption ($E < 8$ kJ mol^{-1}).

4. Results and discussion

4.1. Material characterization

The crude PG was collected from the trunk of peach tree. After purification and drying, PG was grounded into powder before dye adsorption experiments (Fig. 1). The morphology and size of PG particles were observed by optical microscopy (OM) (Fig. 2a). The OM image shows that PG particles are generally spherical shape with sizes in the range of 2–10 μm. From the FTIR spectrum in Fig. 2b, the band at 3420 cm^{-1} is associated with O—H stretching vibration of hydroxyl group; peaks at 2932 and 2865 cm^{-1} come from the C—H stretching vibrations; peak at 1618 cm^{-1} is attributable to the —COO$^-$ stretching which is derived from the uronic acid component (Rosík, Kardošová, & Kubala, 1971); peak at 1074 cm^{-1} is the result of C—O stretching vibration. All these FTIR data are well in accordance with the composition of PG polysaccharide. To gain new information from surface properties of PG

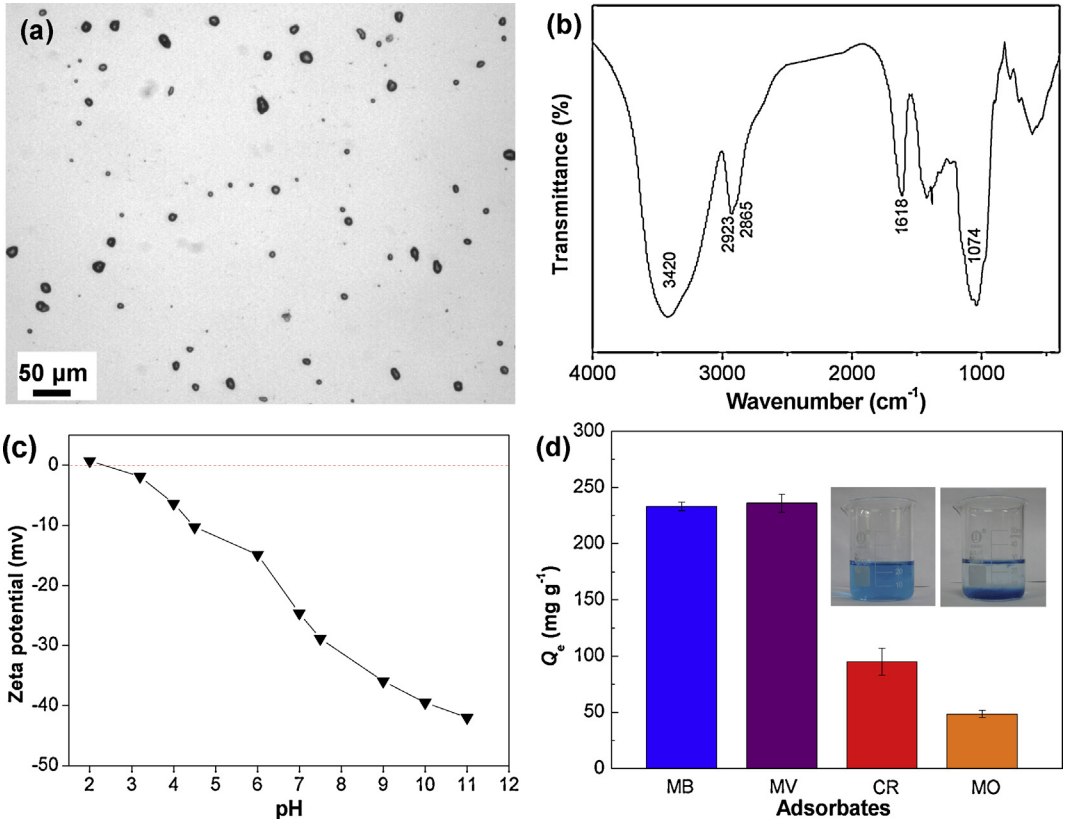

Fig. 2. (a) Optical microscope image of PG particles. (b) FTIR spectrum of PG. (c) Zeta-potential of PG particles as a function of pH. (d) Adsorption capacity of PG for diverse dyes (the initial dye concentration is 1.5 mM). Inset of (d): photograph of MB solution (0.1 mM) before (left) and after (right) adsorption on PG particles.

particles, we measured the values of zeta-potential of PG particles at different pH (Fig. 2c). The isoelectric point (iep) of PG particles is found to occur at pH 2.3. The low iep indicates that the surface of PG is negatively charged in the pH range 3–10 due to the ionization of the carboxylic groups. This negatively charged surface will benefit the sorption of positively charged adsorbates.

4.2. Adsorption performances of PG adsorbent for various dyes

Four kinds of dyes, including methyl violet (MV), methylene blue (MB), methyl orange (MO) and congo red (CR), were chosen to evaluate the adsorption capability of PG (Table 1). Since the adsorption capacity is considered as one of the most critical parameters in practical application, the saturated adsorption capacities of PG for various dyes at high initial dye concentration (1.5 mM) were studied (Fig. 2d). The PG exhibits much higher adsorption capacities for cationic dyes than those of anionic dyes. For MB and MV dyes, the adsorption capacities can reach as high as 233 mg g^{-1} and 237 mg g^{-1}, respectively. At relatively low concentration, the MB could be completely removed from water by PG adsorbent within 3 min as depicted in the inset of Fig. 2d. We speculate that the strong adsorption performance of PG is attributed to the strong interactions between the negatively charged surface —COO^- groups and the positively charged functional groups of dyes such as =N^+H—. Because the CR and MO contain negatively charged —SO_3^- groups (Table 1), their interactions with PG are very weak, resulting in low Q_e for CR and MO. To further understand the adsorption process, MB and MV were selected to investigate the adsorption kinetics and isotherms.

4.3. Adsorption kinetics

The contact time required to reach equilibrium is an important parameter in real applications. In order to establish the time dependence of adsorption, the adsorption of MB and MV solutions (0.4 mM) using PG were studied as a function of contact time (min) and the adsorption capacities of PG at different contact time were determined experimentally. As can be seen in Fig. 3a, the adsorption amounts for both MB and MV increased rapidly in the initial stage in first 5 min, and then slowed down until the adsorption process reached equilibrium in 30 min. About 98% of MB and MV could be adsorbed within the first 5 min. The beginning rapid stage of dye adsorption is due to the surface electrostatic attraction because of the existence of a large number of adsorption sites (e.g., carboxylic groups) on the surface of PG particles. The subsequent slow step is attributable to the limited adsorption sites available on the surface of PG, and the adsorption process followed the intraparticle diffusion mechanism.

To further investigate the adsorption mechanisms, pseudo-first-order and pseudo-second-order kinetic models were used to fit the adsorption data. For pseudo-first-order model, the plot of $\ln(Q_e - Q_t)$ versus t should give a straight line with slope $-k_1$. In fact, however, the correlation coefficients (R^2) for MB and MV are 0.344 and 0.284, respectively (Fig. 3b). Such low correlation coefficients suggested the poor agreement of pseudo-first-order kinetics with the experimental data. In contrast, for pseudo-second-order models, two linear plots of t/Q_t against t give high R^2 of 0.998 and 0.997 for MB and MV, respectively (Fig. 3c). The high correlation coefficients suggest that the pseudo-second-order model is more suitable than pseudo-first-order model for the dye uptake by PG adsorbent. In addition, the plot for intraparticle diffusion model

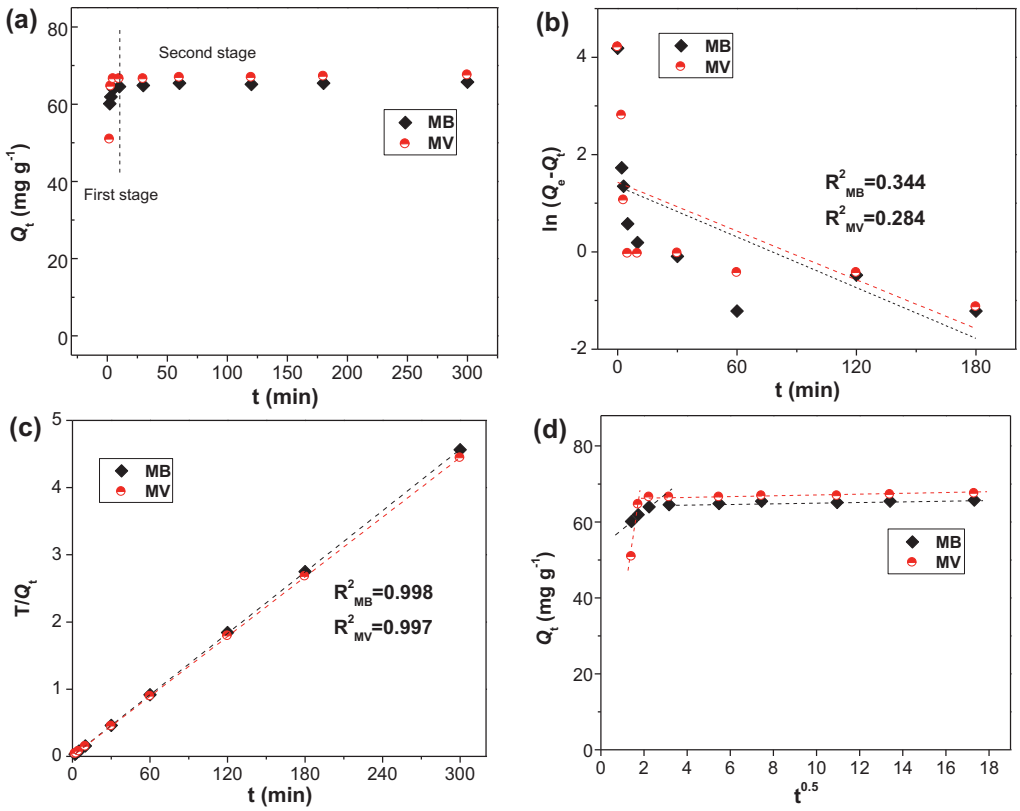

Fig. 3. (a) Effect of contact time on the adsorption of MB and MV by PG at pH 7.0 and 25 °C. The initial concentration of MB or MV is 0.4 mM. Plots of (b) pseudo-first-order, (c) pseudo-second-order and (d) intraparticle diffusion rates for adsorption of MB and MV on PG.

(Fig. 3d) did not pass through the origin implying that the intraparticle diffusion was not the rate controlling factor. Although intraparticle diffusion model was not fitted well to the kinetic data but it followed two distinct linear trends. The first sharp section is the external surface adsorption or instantaneous adsorption stage. The second subdued portion is the gradual adsorption stage, where intraparticle diffusion is rate-controlled. Thus, combination of mechanisms was involved in the adsorption of MB and MV dyes on PG adsorbent.

4.4. Adsorption isotherms

Fig. 4 shows the equilibrium isotherms for the adsorptions of MB and MV. The Freundlich isotherm model can be used to describe a heterogeneous system. The value of lnQ_e against lnC_e according to the experimental isotherm data is shown in the inset of Fig. 4. Table 2 shows the calculated values of isotherm model's parameters. The corresponding R^2 for adsorption of MB and MV are 0.895 and 0.898, respectively. According to Langmuir isotherm model, it assumes that the adsorption occurs at a specific homogenous site within adsorbent, all sites are equivalent and there are no interactions between adsorbate molecules. The plots of C_e/Q_e versus C_e in the inset of Fig. 4 present straight lines with correlation coefficients for MB and MV are 0.978 and 0.965, respectively. Compared with Freundlich isotherm, the Langmuir isotherm better represents the equilibrium adsorption of MB or MV on PG, suggesting that the adsorption process is the monolayer coverage of the dye on the surface of PG adsorbent.

Meanwhile, the values of dimensionless constant separation factor (R_L) calculated from the Langmuir adsorption constant are in the range of 0.17–0.86 and 0.22–0.89 (Table 2), respectively, indicating that the adsorption is a favorable process. In addition, the mean free energy of adsorption (E) values according to the D–R model are 9.13 and 8.78 kJ mol^{-1} for adsorption of MB and MV, respectively, which indicates that chemical-adsorption is the major process involved in the adsorption of MB and MV on PG particles.

The Q_{max} values of MB (298 mg g^{-1}) and MV (277 mg g^{-1}) on PG according to Langmuir isotherm model were compared with those of other bioadsorbents (see Table 3). It can be seen from Table 3 that the Q_{max} value of PG is much higher than those of other adsorbents such as castor seed shell (159 mg g^{-1} for MB), peanut hull (68 mg g^{-1} for MB), rice husk (41 mg g^{-1} for MB), peanut straw char (256 mg g^{-1} for MV), sunflower seed hull (93 mg g^{-1}

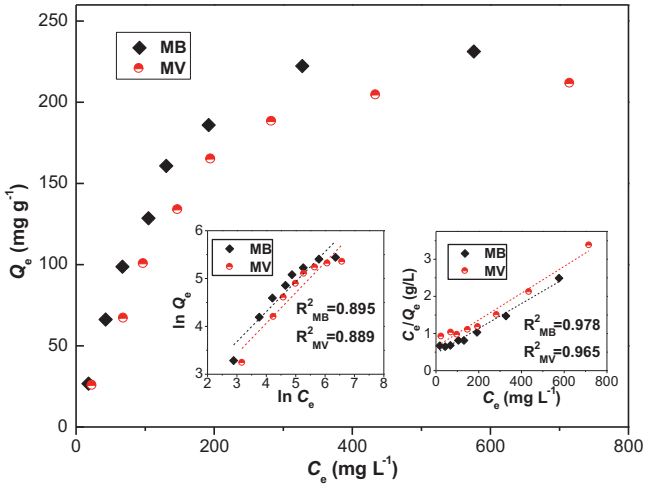

Fig. 4. Adsorption isotherms for the adsorption of MB and MV on PG at pH 7.0 and 25 °C. The insets: the values of lnQ_e against lnC_e based on the Freundlich isotherm model (left) and the linear dependence of C_e/Q_e on C_e based on the Langmuir isotherm model (right).

Table 2
Adsorption parameters of isotherm for the adsorption of MB or MV on PG adsorbent.

	Freundlich isotherm			Langmuir isotherm			
	K_F	b_F	R^2	Q_{max}	K_L	R^2	R_L
MB	6.05	0.625	0.895	298	0.007	0.978	0.17–0.86
MV	4.57	0.636	0.889	277	0.006	0.965	0.22–0.89

Table 3
Comparison of the maximum monolayer adsorption of MB and MV onto various bioadsorbents.

Dye	Adsorbent	Q_{max} (mg g^{-1})	Reference
MB	Castor seed shell	159	Oladoja et al. (2008)
MB	Pineapple stem	119	Hameed, Krishni, Sata (2009)
MB	Coffee husks	90	Oliveira, Franca, Alves, and Rocha (2008)
MB	Peanut hull	68	Gong et al. (2005)
MB	Rice husk	41	Vadivelan and Kumar (2005)
MB	Banana peel	21	Annadurai et al. (2002)
MB	Wheat shell	17	Bulut and Aydin (2006)
MB	Peach gum	298	This study
MV	Peanut straw char	256	Xu, Xiao, Yuan, and Zhao (2011)
MV	Soybean straw char	178	Xu et al. (2011)
MV	Rice hull char	123	Xu et al. (2011)
MV	Sunflower seed hull	93	Hameed (2008)
MV	Mansonia wood sawdust	16	Ofomaja and Ho (2008)
MV	Banana pith	12	Annadurai et al. (2002)
MV	Cellulose-based waste	11	Annadurai et al. (2002)
MV	Peach gum	277	This study

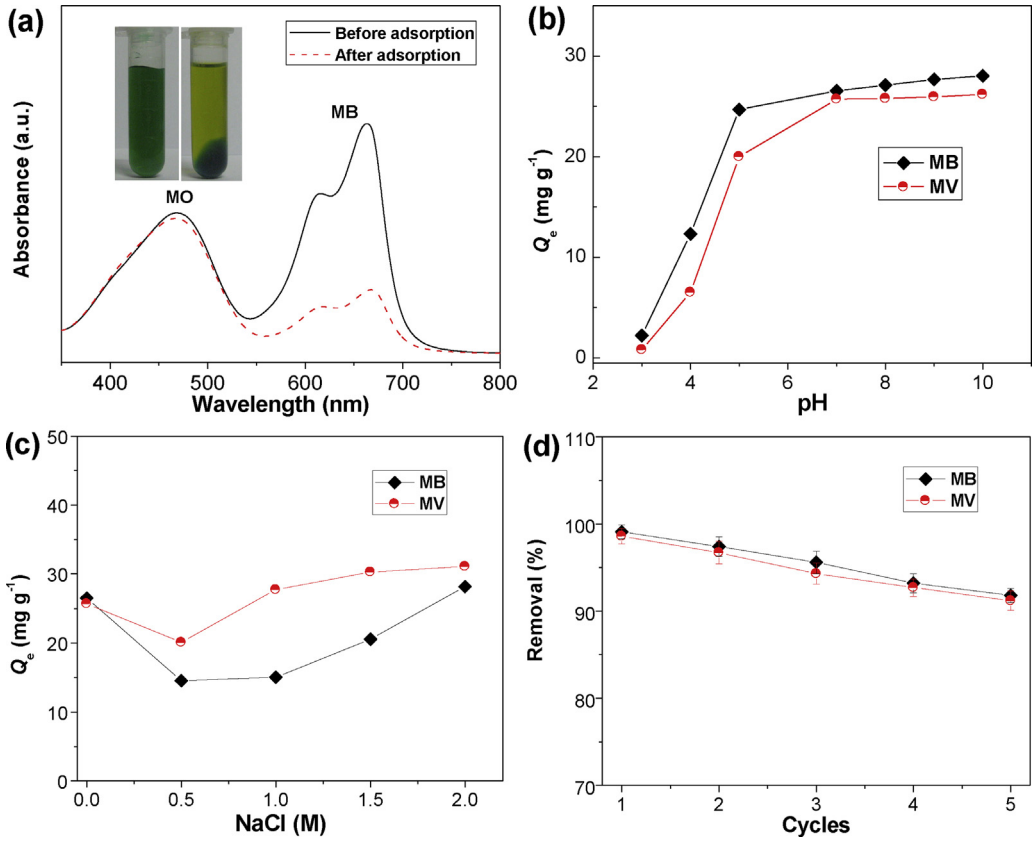

Fig. 5. (a). Absorption spectra of the mixed solution of MB and MO (0.5 mM) before and after adsorption by PG. Inset of (a): photograph of mixed solution of MB and MO before (left) and after (right) adsorption on PG. (b) Effect of pH on the adsorption of MB and MV by PG at 25 °C. (c) Effect of ionic strength on the adsorption of MB and MV by PG at pH 7.0 and 25 °C. (d) Removal efficiency of PG in five successive cycles of desorption-adsorption compared with the original adsorption capacity.

for MV), Mansonia wood sawdust (16 mg g^{-1} for MV), banana pith (12 mg g^{-1} for MV), and so on. Thus, PG is a promising adsorbent for the removal of cationic dyes from wastewaters.

4.5. Selective adsorption

In practical applications, it is very important to separation of specific dye from a mixed solution. Owing to the negative surface of the PG particles over a wide range of pH values, it is possible to selective adsorption of cationic dye from the mixture of dyes. As can be seen in Fig. 5a, the mixture of MB and MO shows two obvious characteristic absorption peaks at 662 nm and 463 nm in the UV–vis absorption spectra, respectively. After the addition of PG, the intensity of peak at 662 nm decreased significantly while no obvious decrease at 463 nm was observed, demonstrated the high selectivity of PG for the adsorption of cationic dye. The high selectivity is possibly due to the fact that the electrostatic attraction between PG and dyes is the main driving force for the adsorption process.

4.6. Influence of pH and ionic strength

Solution pH can affect aqueous chemistry and surface binding sites of the ionic-type adsorbents. To gain further insight into the adsorption process, the effect of initial pH on the adsorption performance of PG was studied from pH 3 to 10 at 25 °C, initial dye concentration of 0.2 mM, adsorbent does of 2 mg mL^{-1} and contact time of 2 h. Fig. 5b shows the adsorption capacities of PG for MB and MV at diverse pH values. With increasing pH from 3 to 10, the adsorption capacities of PG for both MB and MV gradually increase. This is attributed to the fact that the variation of pH can influence the surface charges of PG and the degree of ionization of the dyes. The PG adsorbent is negatively charged in solution due to the presence of numerous carboxylic groups. The decrease of adsorption capacity at very low pH is possibly caused by the protons competition with dye molecules for the available adsorption sites. As the pH increases, the electrostatic attraction between the negatively charged surface of PG and cationic MB or MV molecule enhances, resulting in an increase of adsorption capacity of PG adsorbent.

The influence of ionic strength on the adsorption is shown in Fig. 5c. With increasing the concentration of NaCl, the adsorption capacities for MB and MV firstly decrease and then increase. Generally, when the electrostatic force between the adsorbent surface and dye was attractive, an increase in ionic strength will decrease the adsorption capacity. The increase in dye removal at high concentration of NaCl (e.g., >1.5 M) is caused by an increase in dimerization of dyes in solution, which has been extensively studied by Alberghina, Bianchini, Fichera, & Fisichella, 2000. It has been reported that the high adsorption capacity of dyes under high concentration of NaCl can be attributed to the aggregation of dye molecules induced by the action of salt ions, i.e., salt ions force dyes to aggregate, enhancing the extent of adsorption on adsorbent.

4.7. Regeneration study

For real applications, the regeneration capability of the adsorbent is very important since the dyes can be recovered and the adsorbent can be regenerated for next applications. An excellent adsorbent should not only possess high adsorption capacity, but also high desorption capability in order to significantly reduce the overall cost of the adsorbent. In this work, desorption experiments were conducted in HCl solution (0.05 M) for MB- and MV-adsorbed PG. After desorption, the regenerated PG was reused. Five cycles of desorption-adsorption were performed (Fig. 5d). The regeneration results showed that the adsorption capacity decreased not more than 10% after five cycles of desorption-adsorption compared with the original adsorption capacity.

5. Conclusions

In conclusion, the use of PG as adsorbent for the removal of dyes from aqueous solutions was investigated for the first time. The PG exhibited extraordinary adsorption capacities and high selectivity for cationic dyes such as MB and MV due to the strong electrostatic attraction between its negatively charged carboxylic groups and the positively charged functional groups of dyes. The adsorption rate is fast within 30 min to attain adsorption equilibrium. The adsorption kinetics and isotherms studies demonstrated that the adsorption processes can be well fitted by the pseudo-second-order kinetics and Langmuir isotherm model, respectively. The favorable pH range is 6–10 for adsorption on PG. With increasing the concentration of NaCl, the adsorption capacity of PG firstly decreases and then increases. The PG can be regenerated and used repeatedly. The experimental results imply that the PG may be used as a low cost and promising adsorbent for the efficient removal of cationic dyes from dyeing effluents.

Acknowledgments

The authors appreciate financial support from the National Natural Science Foundation of China (No. 51103028 and No. 21364003), Guangxi Natural Science Foundation (No. 2012GXNSFBA053152), Foundation KH2012YB006, Guangxi Funds for Specially-appointed Expert and Guangxi Small Highland Innovation Team of Talents in Colleges and Universities.

References

Aksu, Z. (2005). Application of biosorption for the removal of organic pollutants: a review. *Process Biochemistry*, *40*, 997–1026.
Alberghina, G., Bianchini, R., Fichera, M., & Fisichella, S. (2000). Dimerization of Cibacron Blue F3GA and other dyes: influence of salts and temperature. *Dyes and Pigments*, *46*, 129–137.
Annadurai, G., Juang, R., & Lee, D. (2002). Use of cellulose based wastes for adsorption of dyes from aqueous solutions. *Journal of Hazardous Materials*, *B 92*, 263–274.
Asgher, M., & Bhatti, H. N. (2012). Evaluation of thermodynamics and effect of chemical treatments on sorption potential of citrus waste biomass for removal of anionic dyes from aqueous solutions. *Ecological Engineering*, *38*, 79–85.
Bulut, Y., & Aydin, H. A. (2006). Kinetics and thermodynamics study of methylene blue adsorption on wheat shells. *Desalination*, *194*, 259–267.
Chen, Z., Zhou, L., Zhang, F., Yu, C., & Wei, Z. (2012). Multicarboxylic hyperbranched polyglycerol modified SBA-15 for the adsorption of cationic dyes and copper ions from aqueous media. *Applied Surface Science*, *258*, 5291–5298.
Chowdhury, S., Mishra, R., Saha, P., & Kushwaha, P. (2011). Adsorption thermodynamics, kinetics and isosteric heat of adsorption of malachite green onto chemically modified rice husk. *Desalination*, *265*, 159–168.
Crini, G. (2006). Non-conventional low-cost adsorbents for dye removal: A review. *Bioresource Technology*, *97*, 1061–1085.
Dotto, G. L., & Pinto, L. A. A. (2011). Adsorption of food dyes onto chitosan: Optimization process and kinetic. *Carbohydrate Polymers*, *84*, 231–238.
Dutta, S., Bhattacharyya, A., Ganguly, A., Gupta, S., & Basu, S. (2011). Application of response surface methodology for preparation of low-cost adsorbent from citrus fruit peel and for removal of methylene blue. *Desalination*, *275*, 26–36.
Fan, W., Gao, W., Zhang, C., Tjiu, W. W., Pan, J., & Liu, T. (2012). Hybridization of graphene sheets and carbon-coated Fe_3O_4 nanoparticles as a synergistic adsorbent of organic dyes. *Journal of Materials Chemistry*, *22*, 25108–25115.
Fernanda, F. S., Philip, A. J. G., Ricardo, W., Guilherme, L. S., Antonio, B., & Marcello, I. (2008). Comparison of structure of gum exudate polysaccharides from the trunk and fruit of the peach tree (*Prunus persica*). *Carbohydrate Polymers*, *71*, 218–228.
Gong, R., Li, M., Yang, C., Sun, Y., & Chen, J. (2005). Removal of cationic dyes from aqueous solution by adsorption on peanut hull. *Journal of Hazardous Materials*, *B 121*, 247–250.
Gupta, V. K., & Suhas. (2009). Application of low-cost adsorbent for dye removal: A review. *Journal of Environmental Management*, *90*, 2313–2342.
Hameed, B. H. (2008). Equilibrium and kinetic studies of methyl violet sorption by agricultural waste. *Journal of Hazardous Materials*, *154*, 204–212.
Hameed, B. H., Krishni, R. R., & Sata, S. A. (2009). A novel agricultural waste adsorbent for the removal of cationic dye from aqueous solutions. *Journal of Hazardous Materials*, *162*, 305–311.

Madaeni, S. S., Jamali, Z., & Islami, N. (2011). Highly efficient and selective transport of methylene blue through a bulk liquid membrane containing Cyanex 301 as carrier. *Separation and Purification Technology*, *81*, 116–123.

Ngah, W. S. W., Teong, L. C., & Hanafiah, M. (2011). Adsorption of dyes and heavy metal ions by chitosan composites: A review. *Carbohydrate Polymers*, *83*, 1446–1456.

Ofomaja, A. E., & Ho, Y. S. (2008). Effect of temperatures and pH on methyl violet biosorption by Mansonia wood sawdust. *Bioresource Technology*, *99*, 5411–5417.

Oladoja, N. A., Aboluwoye, C. O., Oladimeji, Y. B., Ashogbon, A. O., & Otemuyiwa, I. O. (2008). Studies on castor seed shell as a sorbent in basic dye contaminated wastewater remediation. *Desalination*, *227*, 190–203.

Oliveira, L. S., Franca, A. S., Alves, T. M., & Rocha, S. D. F. (2008). Evaluation of untreated coffee husks as potential biosorbents for treatment of dye contaminated waters. *Journal of Hazardous Materials*, *155*, 507–512.

Rafatullah, M., Sulaiman, O., Hashim, R., & Ahmad, A. (2010). Adsorption of methylene blue on low-cost adsorbents: A review. *Journal of Hazardous Materials*, *177*, 70–80.

Rosík, J., Kardošová, A., & Kubala, J. (1971). Infrared spectroscopy of peach-gum polysaccharides of *Prunus persica* (L.) Batsch. *Carbohydrate Research*, *18*, 151–156.

Saha, B., Das, S., Saikia, J., & Das, G. (2011). Preferential and enhanced adsorption of different dyes on iron oxide nanoparticles: A comparative study. *Journal of Physical Chemistry C*, *115*, 8024–8033.

Serpone, N., Horikoshi, S., & Emeline, A. V. (2010). Microwaves in advanced oxidation processes for environmental applications. A brief review. *Journal of Photochemistry and Photobiology C: Photochemistry Reviews*, *11*, 114–131.

Simas, F. F., Gorin, P. A. J., Wagner, R., Sassaki, G. L., Bonkerner, A., & Iacomini, M. (2008). Comparison of structure of gum exudate polysaccharides from the trunk and fruit of the peach tree (*Prunus persica*). *Carbohydrate Polymers*, *71*, 218–228.

Simas-Tosin, F. F., Wagner, R., Santos, E. M. R., Sassaki, G. L., Gorin, P. A. J., & Iacomini, M. (2009). Polysaccharide of nectarine gum exudate: Comparison with that of peach gum. *Carbohydrate Polymers*, *76*, 485–487.

Slokar, Y. M., & Le Marechal, A. M. (1998). Methods of decoloration of textile wastewaters. *Dyes and Pigments*, *37*, 335–356.

Vadivelan, V., & Kumar, K. V. (2005). Equilibrium, kinetics, mechanism, and process design for the sorption of methylene blue onto rice husk. *Journal of Colloid and Interface Science*, *286*, 90–100.

Weber, W. J., & Morris, J. C. (1963). Kinetics of adsorption on carbon from solution. *Journal of the Sanitary Engineering Division*, *89*, 31–59.

Xie, Y., & Ren, S. (2008). Study on fuzzy comprehensive evaluation in optimization for the matrix of peach-gelatin-based microcapsule. *Food Science and Technology*, *9*, 112–116 (in Chinese).

Xie, Y. L., Zhou, H. M., & Qian, H. F. (2006). Effect of addition of peach gum on physicochemical properties of gelatin-based microcapsule. *Journal of Food Biochemistry*, *30*, 302–312.

Xu, R., Xiao, S., Yuan, J., & Zhao, A. (2011). Adsorption of methyl violet from aqueous solutions by the biochars derived from crop residues. *Bioresource Technology*, *102*, 10293–10298.

Zhou, L., Gao, C., & Xu, W. (2010). Magnetic dendritic materials for highly efficient adsorption of dyes and drugs. *ACS Applied Materials & Interfaces*, *2*, 1483–1491.

Zhou, L., He, B., & Huang, J. (2013). Amphibious fluorescent carbon dots: one-step green synthesis and application for light-emitting polymer nanocomposites. *Chemical Communications*, *49*, 8078–8080.

Zou, W., Li, K., Bai, H., Shi, X., & Han, R. (2011). Enhanced cationic dyes removal from aqueous solution by oxalic acid modified rice husk. *Journal of Chemical and Engineering Data*, *56*, 1882–1891.